Proceedings Paper:
Henthorn, S. orcid.org/0000-0003-1913-9283, O'Farrell, T. orcid.org/0000-0002-7870-4097 and Ford, K.L. orcid.org/0000-0002-1080-6193 (2020) Metasurface direct antenna modulators in non-line of sight channels for the Internet of Things. In: 2020 IEEE 31st Annual International Symposium on Personal, Indoor and Mobile Radio Communications. 2020 IEEE 31st Annual International Symposium on Personal, Indoor and Mobile Radio Communications, 31 Aug - 03 Sep 2020, London, UK. IEEE . ISBN 9781728144917

https://doi.org/10.1109/pimrc48278.2020.9217228

Metasurface Direct Antenna Modulators in non-Line of Sight Channels for the Internet of Things

1st Stephen Henthorn
Department of Electronic and Electrical Engineering
University of Sheffield
Sheffield, UK
s.henthorn@sheffield.ac.uk

2nd Timothy O'Farrell
Department of Electronic and Electrical Engineering
University of Sheffield
Sheffield, UK
t.ofarrell@sheffield.ac.uk

3rd Kenneth Lee Ford
Department of Electronic and Electrical Engineering
University of Sheffield
Sheffield, UK
l.ford@sheffield.ac.uk

***Abstract*—A Direct Antenna Modulation (DAM) transmitter is modelled in wideband channels using Direct Sequence Spread Spectrum (DSSS) as a low-cost, low-complexity solution for the Internet of Things (IoT). Metasurface-based DAM is an emerging technique where a baseband signal is modulated directly onto a radio frequency (RF) carrier wave using a reconfigurable metasurface. This technique removes the requirement of the power amplifier (PA) to amplify complex modulated signals, allowing the use of a simple, energy efficient PA to amplify only the carrier wave. The reduction in power consumption and RF electronics makes DAM an attractive low-cost, low-complexity transmitter technology. This paper discusses the use of a DAM transmitter as an IoT access point transmitter using DSSS to overcome broadband fading and mitigate the systematic distortion inherent in the technique. Simulation shows DAM to have negligible impairment in 3GPP urban channels compared with ideal modulation when balanced spreading codes are used.**

***Index Terms*—Internet of Things, Metamaterials, Reconfigurable Intelligent Surfaces, Direct Sequence Spread Spectrum, Direct Antenna Modulation**

I. Introduction

In order to support the increasing numbers of connected devices in the Internet of Things (IoT), two main approaches have been taken. First, new waveforms capable of supporting huge numbers of devices over a large area have been designed, called Low Power Wide Area Networks (LPWAN) [1]. While this allows in the order of 10^4 devices to connect to a single access point, it does not scale for devices requiring greater than 40kbit/s throughput. The second approach has been to densify along with cellular networks, using gaps in LTE spectrum to provide higher data rates with NB-IoT and LTE-M standards [2]. The required waveforms are complex, however, with high peak-to-average power (PAPR) ratios, requiring more expensive radio frequency (RF) electronics in transmitters and reducing their energy efficiency. This places a practical limit on network densification.

Recently, direct antenna modulation (DAM) has been suggested as a novel, low complexity transmitter technology which could enable such densification. In DAM, modulation occurs at transmit power within or after the antenna, rather than in RF electronics at low power. This reduces the amount of RF electronics required, and means the amplification stage only amplifies the carrier wave, rather than complex modulated signals, reducing the complexity and improving the energy efficiency of the power amplifier (PA).

Various techniques have been proposed to achieve DAM, including integrating active components into patch antennas [3] and manipulating the near-field of a passive antenna [4]. One emerging transmitter technology utilises reconfigurable metasurfaces, also known as intelligent surfaces, to perform modulation. Metasurfaces are two-dimensional patterns of conductors where the interaction with incident electromagnetic waves is determined by the geometry of the surface's patterns, and integrating electronic components into the surfaces can then allow these properties to be reconfigured [5]. Through design of these surfaces and choice of signals to bias the components, up to 8PSK modulation has been produced by both reflecting a carrier wave off a surface [6], and transmitting them through a surface [7].

However, to date only line-of-sight (LoS) investigations of the performance of DAM transmitters have been carried out, limiting understanding of their potential application in IoT networks. This is a first investigation of DAM transmitters in dispersive environments. A discussion of transmissive metasurface DAM will be given, allowing construction of a baseband DAM model. This will then be implemented in a simulation of 3GPP channel models, using direct sequence spread spectrum (DSSS) to overcome broadband fading and demonstrate the potential of DAM in realistic channels.

II. Direct Antenna Modulation transmitters

In conventional transmitters, modulation of baseband signals onto a RF carrier wave occurs at low power using a mixer (Fig. 1a). This process is often followed by multiple stages of filtering and amplification, before the entire signal is passed through a PA to produce the final transmitted signal. While this is a robust and flexible architecture, it places particular strain on the PA. Due to having to amplify complex modulated signals, which may have high peak-to-average power ratios, the PA is often complex or has to operate at back-off to avoid

This work was supported in part by Industrial Sponsors NEC Telecom Modus and BT Research through the EPSRC iCASE Award and in part by EPSRC under Grant EP/S008101/1 [Direct Digitisation for Frequency Agile Millimetre Wave Massive MIMO (DD-MaMi)]

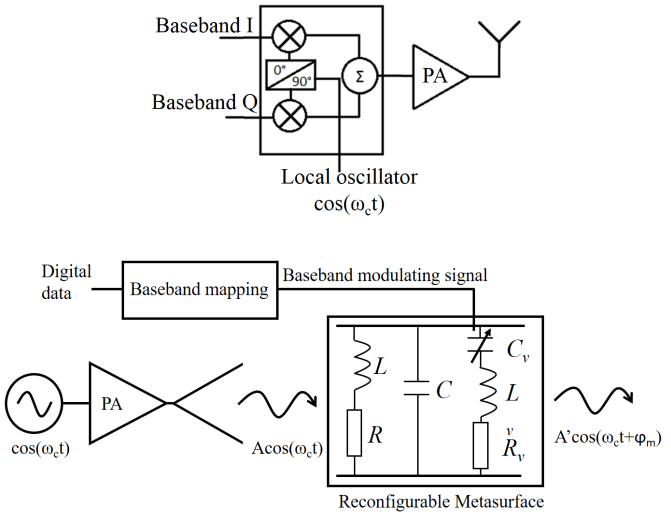

Fig. 1: (a) Block diagram of a conventional homodyne quadrature transmitter, (b) Concept diagram of a DAM transmitter using a transmissive metasurface (FSS)

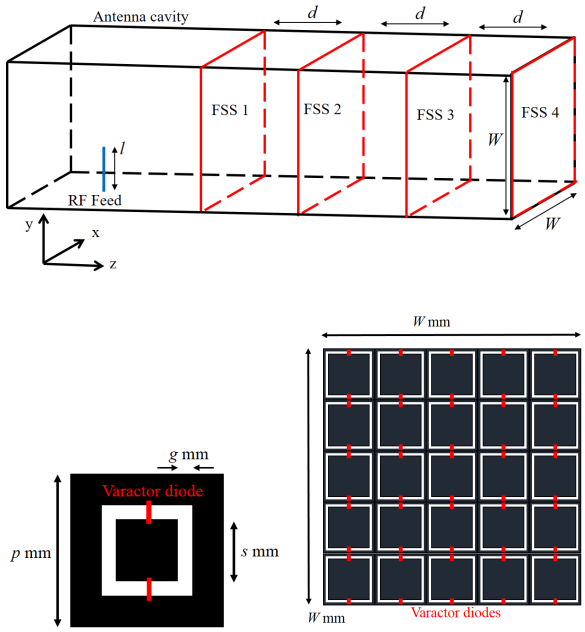

Fig. 2: Diagrams of DAM unit design. (a) Overview, (b) Metasurface unit cell, (c) FSS

distortion, reducing the power efficiency significantly. In modern communications systems this is particularly problematic, with the PAs in LTE base stations being on average 30% efficient and consuming up to 60% of the base station's total power [8], [9].

Metasurface DAM has been suggested as a solution to this problem. By modulating after the PA, only the single-frequency, constant amplitude carrier wave has to be amplified, allowing a simple class D amplifier with theoretical 100% efficiency to be used [10]. As such, DAM transmitters have the potential to be both low complexity and reduce energy usage at base stations significantly, allowing affordable densification of IoT networks.

Fig. 1b shows such a transmitter, with the carrier wave being amplified and passed through a passive antenna element which illuminates a reconfigurable metasurface, here transmissive, which acts as an LC filter. The metasurface is also fed by a baseband signal, which varies the capacitance C_v of variable capacitors integrated into the surface, tuning the filter's centre frequency. This allows control of the transmitted phase ϕ_m, which can be used to produce phase shift keying (PSK) modulation.

The DAM transmitter used in this paper is shown in Fig. 2, and discussed at length in [7]. By using a transmissive metasurface, it becomes possible to integrate the modulating surface and an RF feed into a single unit, ensuring all the fields produced by the feed pass through the metasurface. To ensure 360^o phase change is achievable, four layers of FSS are required, each spaced $d \approxeq \lambda/4$ apart. For this design, which operates at 1.8 GHz, $d = 57$mm, and the RF feed is a monopole of length l=35mm. The metasurface design in Fig. 2c consists of a 5×5 grid of identical unit cells as detailed in Fig. 2b. Each unit cell has two varactor diodes soldered across the centre of the gaps in the conductor, in line with the E-field

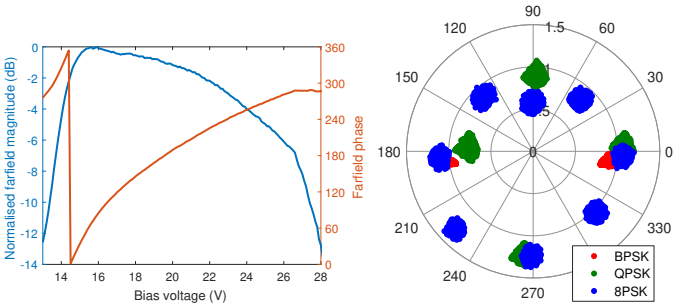

(a) (b)

Fig. 3: Measured DAM transmitter, (a) Normalised farfield magnitude and phase with changing voltage, (b) Constellations produced

produced by the RF excitation.

When biased by a voltage, the diode capacitance changes, tuning the centre frequency of the metasurface filter and so controlling the phase transmitted by the DAM unit (Fig. 3a). PSK constellations can then be created, with each constellation point produced by a different bias voltage (Fig. 3b). However, there is some magnitude variation as the phase changes, due to the roll-off filter response, exacerbated by losses in the metasurface. As such, there is some uncontrollable magnitude variation with changing phase, leading to the distorted constellations in Fig. 3b. Despite this, reasonable bit error rate (BER) performance has previously been shown compared with conventional modulation [7].

TABLE I: Bias voltages for BPSK constellation using DAM

Data	Ideal constellation point	DAM constellation point
0	-1	-0.94
1	1	1.06

TABLE II: Bias voltages for QPSK constellation using DAM

Data	Ideal constellation point	DAM constellation point
00	$e^{-j3\pi/4}$	$1.09e^{-j3\pi/4}$
01	$e^{j3\pi/4}$	$0.89e^{j3\pi/4}$
10	$e^{j\pi/4}$	$1.26e^{j\pi/4}$
11	$e^{-j\pi/4}$	$0.75e^{-j\pi/4}$

TABLE III: Bias voltages for 8PSK constellation using DAM

Data	Ideal constellation point	DAM constellation point
000	1	1.07
001	$e^{j\pi/4}$	$0.84e^{j\pi/4}$
010	$e^{j3\pi/4}$	$0.88e^{j3\pi/4}$
011	$e^{j\pi/2}$	$0.59e^{j\pi/2}$
100	$e^{-j\pi/4}$	$1.05e^{-j\pi/4}$
101	$e^{-j\pi/2}$	$1.23e^{-j\pi/2}$
110	$e^{j\pi}$	$1.12e^{j\pi}$
111	$e^{-j3\pi/4}$	$1.30e^{-j3\pi/4}$

III. Modelling metasurface DAM transmitters

In order to evaluate the performance of metasurface DAM in dispersive channels, a baseband model of FSS modulation was constructed. The key difference between waveforms produced by metasurface DAM and conventional transmitters is the variation in magnitude in relation to the desired phase (Fig. 3a). As this variation is systematic, the magnitude of the waveform produced at each phase in a constellation can be represented as the effective magnitude of the baseband symbol transmitted. This has been carried out using measured data for BPSK (Table I), QPSK (Table II) and 8PSK modulation (Table III). The magnitudes are normalised so the effective constellation power is one Watt for each modulation order. This approach to mapping distortion at chip-level into baseband modelling is a novel approach which has particularly useful application to the systematic distortion of metasurface DAM. In keeping with the measured data, the symbol rate throughout this paper will be 1 MSymbol/s and the carrier frequency, where required, is 1.8 GHz.

All other non-ideal phenomena in the measured performance of metasurface DAM transmitters have been ignored. For example, the measured constellations see a phase offset of up to 5^o from ideal constellation point positions, due to systematic errors in the electronics producing the biasing signal. It is assumed that this can be reduced to negligible levels with appropriate system design. Also, the high error vector magnitude (EVM) shown in Fig. 3b has been shown to be due to systematic errors in the electronics, and reduces notably when spreading codes are used [7]. As such it has been assumed that EVM is purely a product of signal to noise ratio (SNR) in the model.

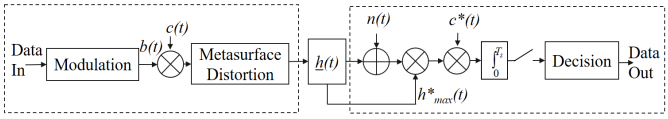

Fig. 4: Schematic of DSSS communications system with a DAM transmitter

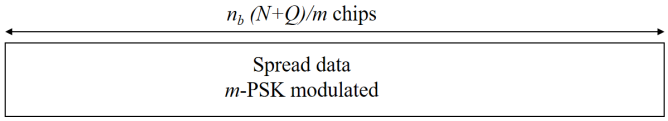

Fig. 5: Packet construction for evaluating DAM DSSS

IV. Simulation of metasurface DAM

This model is then inserted into a baseband simulation of a wireless communications system (Fig. 4). First, a packet of $n_b = 1002$ binary bits is generated. The data is then M-PSK modulated, where M is 2, 4 or 8, to produce $\frac{n_b}{\log_2(M)}$ complex symbols. The stream of symbols $b(t)$ is then multiplied by some spreading code $c(t)$ of length N, resulting in a packet of $\frac{n_b N}{\log_2(M)}$ complex chips (Fig. 5). Each of these complex chips will have one of the values in the 'Ideal constellation point' column of Tables I, II or III. These values are then mapped to the corresponding values in the 'DAM constellation point' column of these tables, providing a baseband representation of metasurface DAM modulation.

This packet of distorted complex chips is then passed through a channel $\underline{h}$. The channels examined in this paper are the ideal LoS case, where $\underline{h} = 1$; the Extended Pedestrian A (EPA) channel developed by 3GPP for LTE applications, with tap delays and relative magnitudes in Table IV; and the Extended Urban (ETU) channel model, with tap delays and relative magnitudes in Table V [11]. In these two non-LoS cases, the specific values of each tap are randomly generated for each packet from a Rayleigh distribution, downsampled using an root raised cosine (RRC) filter of span 6 and roll-off factor 0.25 from a rate of 100 MSample/s to the chip rate of 1 MSample/s, and held constant for the duration of the packet. It is this downsampled channel which is represented by $\underline{h}$. The average downsampled power delay profile for each channel type is shown in Fig. 6. Note that the average sum power in each channel is 1. Additive white Gaussian noise (AWGN) is added at the receiver.

Assuming perfect knowledge of the downsampled channel at the receiver, the maximum tap value of $\underline{h}$ is selected, conjugated and multiplied by the received signal. In frequency selective channels, time diversity is obtained through allowing correlation with the strongest path. The resultant signal is then correlated with the conjugate of the spreading sequence $c^*(t)$, with the output integrated over the length of a symbol. A threshold detector is then used to obtain binary data based on the processed complex signals, allowing BER to be calculated.

TABLE IV: Delay profile of Extended Pedestrian A (EPA) model

Excess tap delay (ns)	Relative power (dB)
0	0.0
30	-1.0
70	-2.0
90	-3.0
110	-8.0
190	-17.2
410	-20.8

TABLE V: Delay profile of Extended Typical Urban (ETU) model

Excess tap delay (ns)	Relative power (dB)
0	-1.0
50	-1.0
120	-1.0
200	0.0
230	0.0
500	0.0
1600	-3.0
2300	-5.0
5000	-7.0

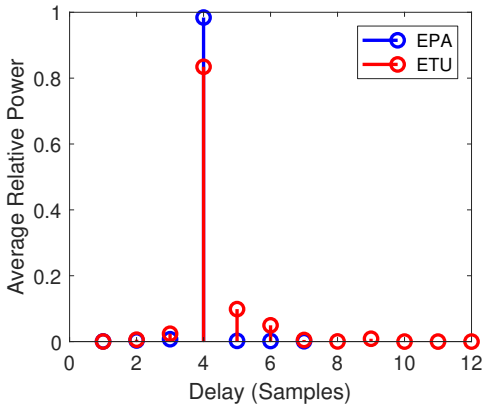

Fig. 6: Downsampled power delay profile for channel models under investigation at 1MSample/s

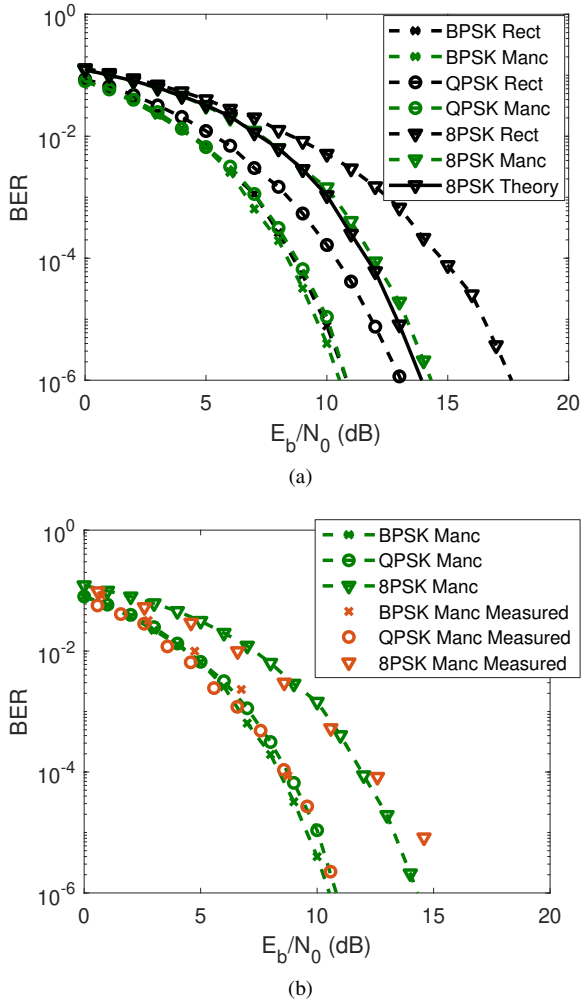

Fig. 7: Simulated BER performance of DAM transmitter producing B, Q and 8PSK modulation in AWGN channel, (a) Simulated with no spreading (Rect) or Manchester code (Manc), (b) Comparison of simulated model with previously measured performance when using Manchester code

This is repeated for each value of $\frac{E_b}{N_0}$ until 500 packet errors have been detected.

A. Performance of narrowband metasurface DAM

To validate the model of metasurface DAM and demonstrate its performance in ideal channels, simulation of the system is performed in an AWGN channel (Fig. 7a). It can be seen that the distortion due to metasurface DAM when no spreading is used, akin to applying a rectangular filter $c(t) = 1$, degrades performance compared with theoretical BER by 3.5dB for 8PSK at an error rate of 10^{-6}. Note that this is largest for 8PSK as its distortion is the most profound. In order to mitigate this distortion, a balanced spreading sequence may be used [7]. By separating each complex symbol into multiple complex chips, which will each be distorted differently by the metasurface modulator, when the chips are correlated with the sequence at the receiver the distortion will be averaged between the different values. This can be seen in Fig. 7b, where improvement of 0.3dB, 2dB and 3dB are achieved for BPSK, QPSK and 8PSK respectively.

For validation of the model, these simulated values were compared with measured results for a metasurface DAM in a LoS channel when a Manchester spreading code is used, found in [7] (Fig. 7b). This shows at most 1.2dB variation from the simulated values, in the 8PSK curve at a BER of 10^{-5}. This small deviation from the measured result is judged to be acceptable, validating the use of this model for further investigation in non-ideal channels.

Application of this model in non-LoS channels, however, demonstrates that the narrowband approach is limited. Simulation of metasurface DAM in the EPA channel model with both no spreading sequence and a Manchester code is shown in Fig. 8. Despite the power delay profile being almost entirely concentrated in a single path, the small amount of intersymbol interference introduced causes an error floor to

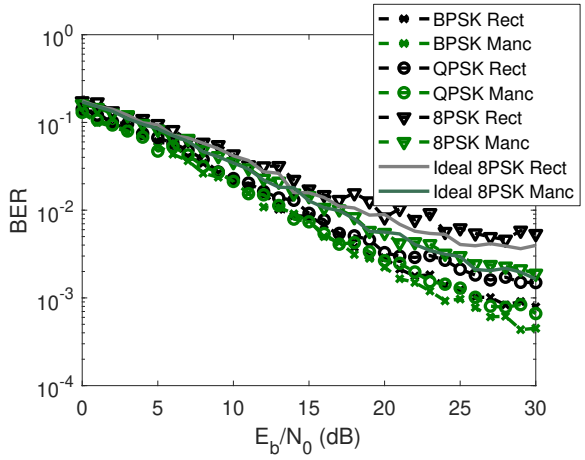

Fig. 8: Simulated BER performance of DAM transmitter producing B, Q and 8PSK modulation in EPA channel with no spreading (Rect) or Manchester code (Rect)

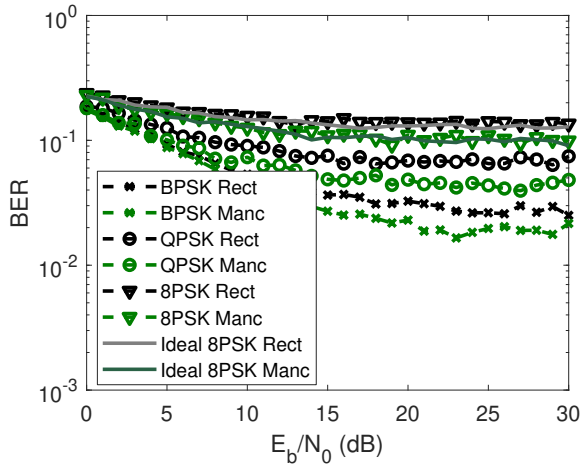

Fig. 9: Simulated BER performance of DAM transmitter producing B, Q and 8PSK modulation in ETU channel with no spreading (Rect) or Manchester code (Rect)

be reached when no spreading sequence is used, at 8×10^{-4} for BPSK, 1×10^{-3} for QPSK and 5×10^{-3} for QPSK. Use of the Manchester spreading code slightly improves performance, particularly at 8PSK where the error floor is reduced to 1×10^{-4}, due to mitigating the distortion introduced by metasurface DAM modulation. The poor autocorrelation properties of the Manchester code add little mitigation of the intersymbol interference. Simulated 8PSK with the ideal constellation described in the second column of Table III in the same channel is also shown for comparison, and demonstrates little deviation with the simulated distorted performance when the Manchester spreading code is used, suggesting little is lost in performance from using the low complexity, energy efficient metasurface DAM transmitter in this scenario. However, the overall error performance is poor.

This performance is further degraded in more dispersive channels such as the ETU at 1MSymbol/s, which has 4

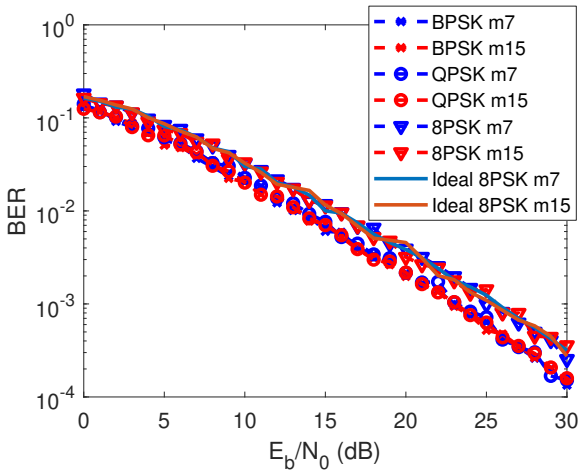

Fig. 10: Simulated BER performance of DAM transmitter producing B, Q and 8PSK modulation in EPA channel with length 7 m-sequence (b7) or length 15 m-sequence (m15)

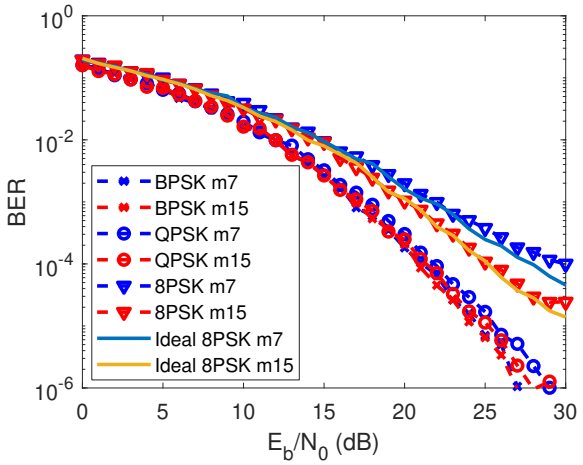

Fig. 11: Simulated BER performance of DAM transmitter producing B, Q and 8PSK modulation in EPA channel with m-sequence of length 7 (b7) or length 15 m-sequence (m15)

significant paths (Fig. 9). With no spreading sequence, an error floor of 0.025 is reached for BPSK, 0.075 for QPSK and 0.15 for 8PSK due to the intersymbol interference introduced. Using a Manchester code again provides some improvement, bring QPSK to an error floor of 0.05 due to mitigating the distortion introduced by metasurface DAM and some slight protection against intersymbol interference, but the overall performance is poor. Once again, simulation of an ideal transmitter is included, showing only slight degradation in performance from using the low complexity metasurface DAM transmitter. This demonstrates that relying on the narrowband transmission schemes investigated previously in the literature for transmission in non-LoS channels leads to unsatisfactory performance.

B. Metasurface DAM with binary spreading codes

In order to overcome this, DSSS with binary spreading codes was investigated with metasurface DAM transmitters. Fig. 10 shows BER curves for metasurface DAM transmitters in the EPA channel model using the length 7 m-sequence code, [1,1,1,-1,-1,1,-1], and the length 15 m-sequence, [1,-1,-1,1,1,-1,1,-1,1,1,1,1,-1,-1,-1]. Note that both codes are in their least-sidelobe-energy rotation [12], [13]. For all modulation orders, the error rate becomes reducible below 10^{-4} and beyond, allowing the use of these transmitters in such channels. However, while both the length 7 and the length 15 m-sequence mitigate the intersymbol interference introduced by the channel, the interfering paths do not introduce much opportunity for diversity gain due to their low average powers. As such high $\frac{E_b}{N_0}$ values are required to reach low BERs. Again ideal 8PSK modulation is compared with metasurface DAM performance, with both the length 7 and the length 15 m-sequence giving no observable degradation. This shows that pseudobalanced codes perform almost as well as perfectly balanced codes in mitigating the distortion introduced by metasurface DAM, while their autocorrelation properties allow exploitation of diversity in dispersive channels.

This is further emphasised when the ETU channel model is explored, which is more dispersive than the EPA channel model (Fig. 11). Both BPSK and QPSK reach below 10^{-6} BER between 28dB and 30dB $\frac{E_b}{N_0}$ for both the length 7 and the length 15 m-sequence. The latter achieves up to 1dB gain compared with the former, suggesting little improvement from the loss in spectral efficiency required. However, 8PSK reaches an error floor of 1×10^{-4} with the length 7 m-sequence and 2×10^{-5} with the length 15 m-sequence. This suggests a longer code is necessary to reduce BER performance below 10^{-6} with 8PSK modulation. Further, ideal 8PSK modulation achieves error floors of 4×10^{-5} and 1×10^{-5}, showing that slightly less loss in performance by metasurface DAM compared with ideal modulation is achieved using longer pseudobalanced codes, as they mitigate the distortion more effectively. However, the difference is small. In all, this investigation demonstrates the low complexity and energy efficient characteristics of metasurface DAM transmitters can be exploited in non-LoS channels by using short balanced spreading codes which both mitigate the distortion introduced by metasurface DAM modulation, and allow exploitation of time diversity to improve error rates.

V. Conclusions

The performance of low complexity metasurface DAM transmitters has been modelled in non-LoS wireless channels. Using a novel baseband model of the distortion introduced by metasurface DAM as a technique, simulations were performed in 3GPP EPA and ETU channels. It was found that narrowband approaches perform poorly, as previous use of a Manchester code to overcome the systematic distortion caused by metasurface DAM is ineffective in dispersive channels. However, use of DSSS with short binary spreading codes allows the exploitation of diversity in these channels, obtaining BERs of below 10^{-6} at 28dB $\frac{E_b}{N_0}$ values, while mitigating the distortion such that negligible degradation was experienced by 8PSK in the ETU channel compared with ideal modulation when pseudobalanced codes were used. This demonstrates the potential use of low complexity, energy efficient metasurface DAM transmitters in real-world applications such as IoT networks. Future work will intestigate the performance of metasurface DAM with DSSS over frequency selective channels with a RAKE receiver.

References

[1] U. Raza, P. Kulkarni, and M. Sooriyabandara, "Low power wide area networks: An overview," *IEEE Communications Surveys & Tutorials*, vol. 19, no. 2, pp. 855–873, 2017.

[2] M. R. Palattella, M. Dohler, A. Grieco, G. Rizzo, J. Torsner, T. Engel, and L. Ladid, "Internet of things in the 5G era: Enablers, architecture, and business models," *IEEE Journal on Selected Areas in Communications*, vol. 34, no. 3, pp. 510–527, 2016.

[3] M. Salehi and M. Manteghi, "A new technique for high data-rate transmission using narrowband antennas," in *Antennas and Propagation Society International Symposium (APSURSI), 2014 IEEE*, Conference Proceedings, pp. 573–574.

[4] A. Babakhani, D. B. Rutledge, and A. Hajimiri, "Near-field direct antenna modulation," *Microwave Magazine, IEEE*, vol. 10, no. 1, pp. 36–46, 2009.

[5] G. Oliveri, D. H. Werner, and A. Massa, "Reconfigurable electromagnetics through metamaterials—a review," *Proceedings of the IEEE*, vol. 103, no. 7, pp. 1034–1056, 2015.

[6] W. Tang, J. Y. Dai, M. Chen, X. Li, Q. Cheng, S. Jin, K. Wong, and T. J. Cui, "Programmable metasurface-based RF chain-free 8PSK wireless transmitter," *Electronics Letters*, vol. 55, no. 7, pp. 417–420, 2019.

[7] S. Henthorn, K. L. Ford, and T. O'Farrell, "Direct antenna modulation for high-order phase shift keying," *IEEE Transactions on Antennas and Propagation*, vol. 68, no. 1, pp. 111–120, 2020.

[8] A. Arbi, T. O'Farrell, F.-C. Zheng, and S. C. Fletcher, "Toward green evolution of cellular networks by high order sectorisation and small cell densification," in *Interference Mitigation and Energy Management in 5G Heterogeneous Cellular Networks*, C. Yang and J. Li, Eds. IGI Global, 2016.

[9] G. Auer, V. Giannini, C. Desset, I. Godor, P. Skillermark, M. Olsson, M. A. Imran, D. Sabella, M. J. Gonzalez, O. Blume, and A. Fehske, "How much energy is needed to run a wireless network?" *IEEE Wireless Communications*, vol. 18, no. 5, pp. 40–49, 2011.

[10] S. C. Cripps, *RF Power Amplifiers for Wireless Communications, Second Edition (Artech House Microwave Library (Hardcover))*. Artech House, Inc., 2006.

[11] "LTE; Evolved Universal Terrestrial Radio Access (E-UTRA); User Equipment (UE) radio transmission and reception," 3GPP, Standard, Apr. 2017.

[12] H. Donelan and T. O'Farrell, "Families of ternary sequences with aperiodic zero correlation zones for MC-DS-CDMA," *Electronics Letters*, vol. 38, no. 25, pp. 1660–1661, Dec 2002.

[13] T. O'Farrell, "Spread spectrum communication," Jan. 30 2001, US Patent 6,181,729. [Online]. Available: https://www.google.ch/patents/US6181729